"Giant Surfactants" Created by the Fast and Efficient Functionalization of a DNA Tetrahedron with a Temperature-Responsive Polymer

Thomas R. Wilks,[†] Jonathan Bath,[‡] Jan Willem de Vries,[§] Jeffery E. Raymond,[⊥] Andreas Herrmann,[§] Andrew J. Turberfield,[‡] and Rachel K. O'Reilly[†,*]

[†]Department of Chemistry, University of Warwick, Coventry, West Midlands CV4 7AL, U.K., [‡]Department of Physics, University of Oxford, Clarendon Laboratory, Parks Road, Oxford, OX1 3PU, U.K., [§]Department of Polymer Chemistry, Zernike Institute for Advanced Materials, University of Groningen, Nijenborgh 4, Groningen, 9747 AG Groningen, The Netherlands, and [⊥]Laboratory for Synthetic-Biologic Interactions, Texas A&M University, POB 30012, College Station, Texas 77842-3012, United States

ABSTRACT Copper catalyzed azide—alkyne cycloaddition (CuAAC) was employed to synthesize DNA block copolymers (DBCs) with a range of polymer blocks including temperature-responsive poly(*N*-isoproylacrylamide) (poly(NIPAM)) and highly hydrophobic poly(styrene). Exceptionally high yields were achieved at low DNA concentrations, in organic solvents, and in the absence of any solid support. The DNA segment of the DBC remained capable of sequence-specific hybridization: it was used to assemble a precisely defined nanostructure, a DNA tetrahedron, with pendant poly(NIPAM) segments. In the presence of an excess of poly(NIPAM) homopolymer, the tetrahedron—poly(NIPAM) conjugate nucleated the formation of large, well-defined nanoparticles at 40 °C, a temperature at which the homopolymer precipitated from solution. These composite nanoparticles were observed by dynamic light scattering and cryoTEM, and their hybrid nature was confirmed by AFM imaging. As a result of the large effective surface area of the tetrahedron, only very low concentrations of the conjugate were required in order for this surfactant-like behavior to be observed.

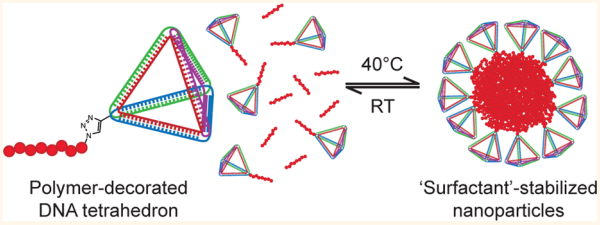

KEYWORDS: DNA · polymers · temperature responsive · surfactants · nanoparticles

Over the past two decades, interest in and, perhaps more importantly, applications of nanotechnology have blossomed. One important contributing factor was the introduction by Seeman of structural DNA nanotechnology[1] and the further development of techniques such as Rothemund's DNA origami,[2] which have enabled the facile production of a wide variety of precisely defined nanoscale objects. These structures made of biomolecules can be engineered using common biochemical tools and made responsive to a range of useful stimuli such as pH,[3,4] temperature, enzymatic action, and the presence or absence of small fragments of DNA or RNA.[5,6] DNA nanostructures can exhibit novel crystallization behavior,[7,8] deliver drug molecules to specified target sites,[9] and have the ability to perform complex computational tasks.[10,11]

In parallel to the rise of DNA as a nanoscale building material, the proliferation of controlled radical polymerization (CRP) techniques has given materials scientists an unprecedented degree of control over the structure and composition of synthetic polymers.[12−14] Amphiphilic diblock copolymers, polymers containing two distinct domains, one hydrophobic and one hydrophilic, covalently joined together, are of particular interest as they are also capable of self-assembly in aqueous solutions to form nanoscale structures of precise size and shape. Spherical, cylindrical[15,16] and vesicular morphologies[17] are all readily accessible. The size of these structures can be relatively easily tuned by altering the lengths of the polymer segments. Synthetic polymers are available that are responsive to a huge range of stimuli including light, temperature and pH: the corresponding

* Address correspondence to rachel.oreilly@warwick.ac.uk.

Received for review May 24, 2013 and accepted September 16, 2013.

Published online September 16, 2013
10.1021/nn402642a

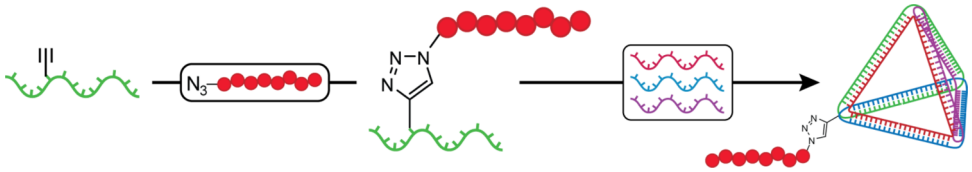

Figure 1. The strategy used to synthesize the tetrahedron–polymer conjugate: attachment of the polymer to one of the component strands, followed by assembly of the tetrahedron.

nanostructures can therefore also be tailored to respond to these environmental cues.[18–20]

Both approaches have their drawbacks. DNA is expensive to produce, and its responsiveness to different stimuli is limited; polymers lack the structural programmability of DNA and its precision of synthesis. Recently, a number of research groups have explored the possibility of combining the two, to produce hybrid DNA–polymer materials. Herrmann *et al.* have synthesized amphiphilic DNA block copolymers (DBCs) by attaching poly(propylene oxide) (PPO) to a short piece of single stranded DNA (ssDNA).[21,22] The hydrophobic PPO segment directs the material to self-assemble in aqueous solution into well-defined micelles with ssDNA in the corona. The ssDNA may then hybridize with a complementary strand, which can be modified to bear a particular targeting ligand or reactive group, lending the micellar scaffold a modular character.[21,23,24] The Mirkin group has used DNA as a reversible cross-linker between organic and inorganic nanostructures.[25] Gianneschi *et al.* have used DBCs to create nanostructures that can switch morphology in response to enzymatic action and the addition/removal of complementary ssDNA.[26] pH-induced phase transitions of DBCs between spherical micelles and nanofibers were realized by Liu *et al.*[27] Most recently, Sleiman *et al.* have used DBCs to make DNA nanofibers with periodically spaced polymer domains arranged along them.[28,29] Each approach has its own unique points of interest: Herrmann's work emphasizes how useful it can be to incorporate a new interaction (that of DNA hybridization) into a polymer nanostructure; Gianneschi's demonstrates how incorporation of DNA allows one to manipulate nanoscale polymeric materials using biological tools; Liu's emphasizes the use of external stimuli in similar processes; and Sleiman's approach highlights DNA's ability to impart highly reproducible, long-range order.

These studies clearly demonstrate the huge potential that DBCs have for the creation of novel, functional materials; however, the synthesis of DBCs is typically nontrivial, especially when the polymer segment has some degree of hydrophobic character, and yields are normally low. Because of this, the field is still small. The variety of polymers in DBCs remains limited, and the ability of the DNA segment to form complex structures is relatively under-exploited.

The principal aims of this work were to identify a fast, efficient and accessible solution-based synthetic method for the production of DBCs; to use this method to attach a responsive polymer to a DNA strand; to form polymer-decorated DNA nanostructures from the resulting DBC conjugate; and to study the temperature-responsive behavior of this conjugate in solution.

Because of its compatibility with a wide range of functional groups and its ability to polymerize, with control, a large variety of different monomers, reversible addition–fragmentation chain transfer (RAFT) polymerization was chosen to synthesize the polymers for this study.[14] A DNA tetrahedron was identified as the target nanostructure as it is straightforward to assemble.[30] The aim was to attach polymers to appropriate component strands of DNA, and then assemble the tetrahedron (Figure 1). This approach has the advantage that only one coupling chemistry is needed to attach any number of different polymers to the DNA structure; if the polymers were to be attached to a preassembled DNA structure, a separate, orthogonal conjugation chemistry would be required for each polymer, which would rapidly become impractical.

RESULTS AND DISCUSSION

Polymers bearing a terminal azide group were synthesized by RAFT polymerization. Initially, the synthesis was attempted using an azide-containing chain transfer agent (CTA) (Figure S1, Supporting Information, **2**). However, FTIR revealed that the azide group had to a large extent degraded, which was in agreement with a previous report.[31] It was necessary, therefore, to adopt a postpolymerization functionalization approach, which afforded polymers with a much higher percentage incorporation of the azide (Figure S2, Supporting Information). CTA **1** was synthesized and used to produce poly(NIPAM) with a terminal pentafluorophenyl (PFP) ester group,[32] which, following removal of the trithiocarbonate group with α,α′-azoisobutyronitrile (AIBN) and lauroyl peroxide (LPO),[33] was then available for substitution with 1-azido-3-aminopropane. ^{1}H NMR spectroscopy confirmed the formation of the amide: the CH_2 signals adjacent to the azide and amide are clearly observable, both at around 3.30–3.40 ppm (see Figure 2). IR analysis further confirmed the presence of the azide group (see Figure S2, Supporting Information). Three poly(NIPAM)-N_3 samples were prepared with different molecular weights (see Table 1); all were purified by extensive dialysis (MWCO = 1000 Da) against 18 MΩ water.

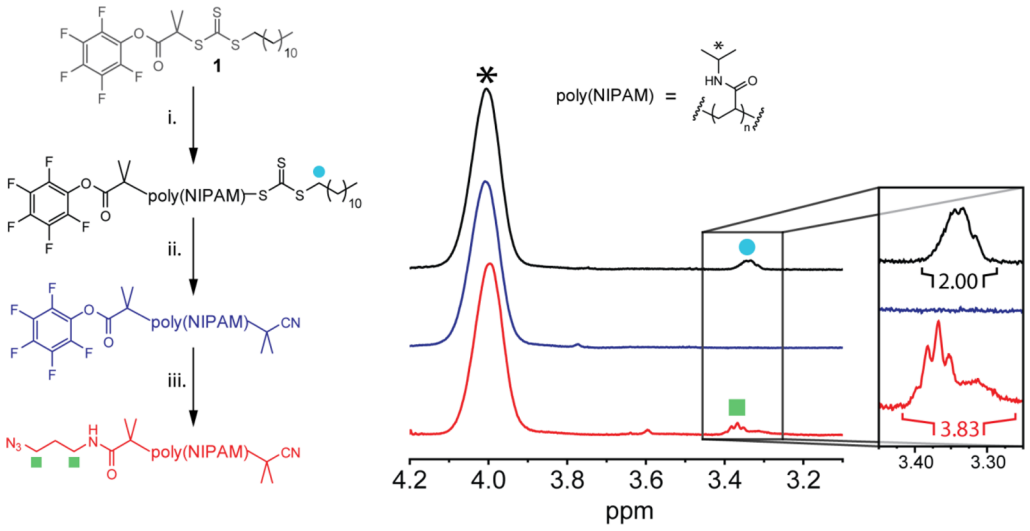

Figure 2. ^{1}H NMR spectra showing removal of the trithiocarbonate group and subsequent substitution of the PFP activated ester to introduce an azide moiety. Reaction conditions: (i) NIPAM (100 equiv w.r.t. 1), AIBN (0.1 equiv), 1,4-dioxane (1.5 mL per gram of monomer), N_2, 65 °C, 2 h; (ii) AIBN (100 equiv), LPO (4 equiv), toluene, N_2, 80 °C, 5 h; (iii) 3-azido-1-aminopropane (5 equiv), TEA (2.5 equiv), THF, 35 °C to RT, 17 h.

TABLE 1. Properties of the Polymers Synthesized for This Work

polymer	type	M_n^{NMR}/kDa[a]	M_w/M_n[b]
P1a	poly(NIPAM)$_{45}$-N_3	5.3	1.07
P1b	poly(NIPAM)$_{90}$-N_3	10.4	1.09
P1c	poly(NIPAM)$_{173}$-N_3	19.8	1.09
P2	poly(NIPAM)-C≡CH	7.3	1.16
P3	poly(styrene)-C≡CH	4.4	1.12
P4	poly(DMA)-N_3	7.2	1.09
P5	poly(4-AM)-N_3	13.8	1.11

[a] Determined from the ratio of the integrated signal from the polymer end groups and the polymer NHC*H* signal in the ^{1}H NMR spectrum. [b] Determined by DMF SEC using PMMA calibration standards.

A sample of poly(NIPAM) containing a terminal alkyne group (Table 1, **P2**) was also synthesized by RAFT using a previously reported CTA (Figure S1, Supporting Information, **3**).[34]

Poly(NIPAM) is well-known for its temperature-responsive character: it typically exhibits a cloud point around 32 °C in aqueous solution.[35,36] It has previously been combined with oligonucleotides and the hybrids utilized for the thermally induced purification of plasmid DNA, PCR amplicons, genotoxins, and DNA binding proteins.[21,37−41] There has also been a recent report indicating that the cloud point of DBCs containing poly(NIPAM) can be modulated by the hybridization of complementary DNA.[42] The cloud point of the poly(NIPAM)$_{45}$ (Table 1, **P1a**) synthesized for this work was measured to be 42 °C at a concentration of 0.8 mg mL^{-1} in TEM buffer (100 mM Tris HCl pH 8.0, 1 mM EDTA, 6 mM $MgCl_2$) (see Figure S3, Supporting Information). This higher value can be attributed to the low molecular weight of the polymer and the relatively hydrophilic end groups.

One aim of this work was to identify a reliable method of conjugating polymers to DNA in a principally organic milieu. The copper-catalyzed azide alkyne cycloaddition (CuAAC) has been extensively used in aqueous media to achieve efficient macromolecular coupling,[43] including DNA−DNA coupling and nucleotide modification (as exemplified by the work of Brown *et al.*[44,45]), but it has been less successful in organic solvents compatible with hydrophobic polymers. It has been suggested that the formation of the active copper species is much more difficult in these systems because of the strongly coordinating nature of the solvent,[46] so with this is in mind we set out to test a variety of catalyst combinations in the hope of identifying one that would be effective for DNA−polymer conjugation. The solvents *N*,*N*-dimethylformamide (DMF), dimethylsulfoxide (DMSO), and tetrahydrofuran (THF) were all tested. The reaction between a 22 nt strand with a 5′ azide modification (s0-azide; see below for DNA sequences) and **P2** (Table 1), which contained a terminal alkyne group, was used for all catalyst testing.

Of the catalysts tested (Table S1 and Figure S4, Supporting Information), only one was found to be effective in producing the desired product: copper iodide triethylphosphite (CuI·P(OEt)$_3$). This species contained a precomplexed copper(I) center, so the active catalyst was already formed when the solution was added to the reaction mixture. In the case of every other catalyst investigated, the active species was formed *in situ*: we believe that the low rate for this step reduced the efficiency of the reaction.

A number of control experiments were carried out to confirm that the band due to the conjugate had been correctly identified (Figure S5, Supporting Information, lanes 1−5). These showed that there was no association

between the polymer and DNA in the absence of catalyst, that the polymer did not bind the PAGE stain, that the catalyst did not cause degradation or aggregation of the DNA, and that no reaction occurred between the DNA and the polymer when the azide group was missing from the former. These results conclusively showed that the new bands indicated in Figures S4 and S5 (Supporting Information) were indeed due to the DNA–polymer conjugate.

Further optimization of the conjugation conditions was carried out: it was found that DMF, DMSO, and 1-methyl-2-pyrrolidinone (NMP) were all effective solvents for the reaction. Increasing the equivalents of catalyst and polymer used also increased the efficiency, with yields for the fully optimized reaction reaching between 70 and 90% (as assessed by PAGE densitometry of the crude reaction mixtures, see Figure S5, Supporting Information). These are some of the highest yields ever reported for DNA–polymer conjugation in solution. (In previously reported syntheses of linear DBCs containing the polymer block poly(NIPAM) in aqueous solution, conjugation efficiencies were generally low, ranging from 15 to 40%.[37,47]) For internal modifications of DNA with poly(NIPAM), described below, coupling yields were considerably lower, only reaching 2.5–6.5%.[38] The reaction procedure described above can be carried out at room temperature (so there is very little solvent evaporation, important when working with such low volumes), at high dilution (the DNA in the test reactions was at 10 μM), and over a relatively short time (incubation overnight). No DNA synthesis equipment or other specialized equipment is required.

Having established an effective catalyst system, the positions of the azide and alkyne groups were switched (because internal modification of DNA sequences with an alkyne is more straightforward, and less expensive, than with an azide). As Figure S6 (Supporting Information) shows, this made no difference to the efficiency of the reaction. It was found, however, that degassing of the reaction solvent was necessary to prevent Glaser coupling of the alkyne-functionalized DNA strands (Figure S7, Supporting Information); this was accomplished by simply bubbling with nitrogen for thirty minutes.

To emphasize the versatility of this coupling chemistry, three further DBCs were synthesized (**P3**–**5**, Table 1). Poly(dimethylacrylamide) (poly(DMA)) and poly(4-acryloylmorpholine) (poly(4-AM)) are both permanently hydrophilic polymers with potential applications as biocompatible "stealth" coatings for drug delivery vehicles. Both were synthesized with a terminal azide group as described above and conjugated to alkyne-functionalized DNA in approximately 50% yield with no further optimization of the reaction conditions (see Figure S8, Supporting Information). Poly(styrene) is a highly hydrophobic polymer, and its conjugation to DNA has previously been realized in only low yields

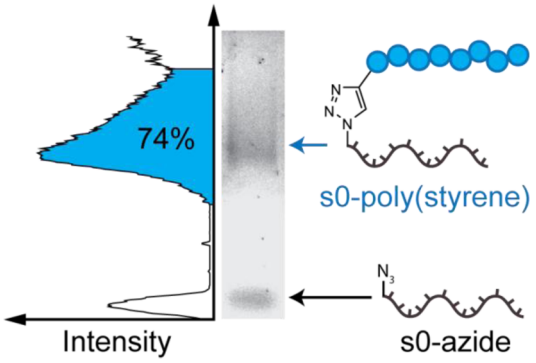

Figure 3. 2% agarose gel analysis of a poly(styrene)–DNA conjugate synthesized using CuAAC in DMF (densitometry plot shown to left of gel).

using solid phase synthesis.[48] Using our CuAAC technique, alkyne-functionalized poly(styrene) was successfully conjugated to azide-functionalized DNA in 74% yield (Figure 3), an unprecedented efficiency for the conjugation of a hydrophobic polymer to DNA in solution.

It was hypothesized that, in accordance with a previous report,[25] the amphiphilic DNA–poly(styrene) conjugate may form micellar structures in aqueous solution. A solution of DNA–poly(styrene) conjugate in DMF was therefore diluted by a factor of 5 with 18 MΩ water then analyzed by Dynamic Light Scattering (DLS). After filtration through a 0.22 μm cellulose acetate membrane to remove insoluble material, nanoparticles were observed (see Figure S9, Supporting Information). These particles were imaged by TEM, dry on a graphene oxide support, without staining.[49] Well-defined nanoparticles with diameters around 20 nm were observed, confirming the amphiphilic nature of the DNA–poly(styrene) conjugate (see Figure 4 and Supporting Information).

In order to construct the polymer-functionalized DNA tetrahedron, it was first necessary to synthesize DBCs containing an oligonucleotide with the appropriate base sequence. The s2 tetrahedron component strand[30] was purchased containing an alkyne-modified U in place of A12, an unhybridized "hinge" base joining double-stranded edges at a vertex of the assembled tetrahedron. This internally modified strand (s2-alkyne), which is more challenging to modify, was conjugated to P1a–c with efficiencies of up to 74% as shown in Figure 5. The conjugates were purified by HPLC (see Figure S10, Supporting Information).

The published procedure for assembly of DNA tetrahedra requires that the four component strands (s1–4) be mixed and heated to 95 °C.[30] Since the poly(NIPAM) used in this study had a lower critical solution temperature (LCST) of 42 °C (see above) it was desirable to avoid the use of heat as a denaturant. An isothermal assembly strategy was therefore adopted, as described previously by Simmel *et al.*[50] Equimolar amounts of s1, s2-poly(NIPAM)$_{45}$, s3, and s4 were mixed in 85% formamide at a concentration of 100 nM. The solution

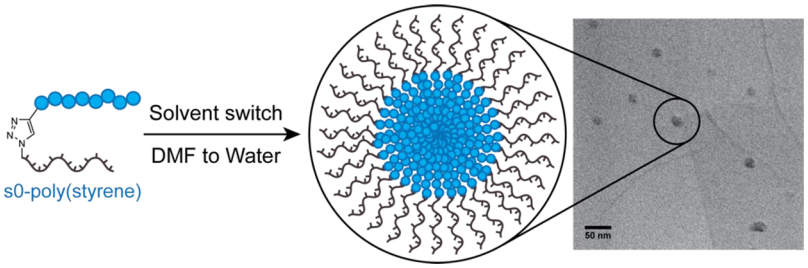

Figure 4. TEM micrograph of nanoparticles formed when the DNA–poly(styrene) conjugate was transferred from DMF (a good solvent for both blocks) to water (a poor solvent for poly(styrene)). The sample was dried directly onto the graphene oxide-coated TEM grid without staining. Scale bar: 50 nm.

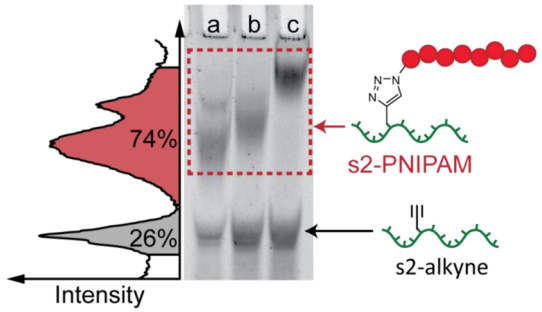

Figure 5. DBCs containing the tetrahedron s2 strand. 15% native PAGE analysis of crude reaction mixtures from the synthesis of lane a, s2-PNIPAM$_{45}$ (densiometry plot shown to left of gel); lane b, s2-PNIPAM$_{90}$; lane c, s2-PNIPAM$_{173}$.

was transferred to a microdialyzer fitted with a 1000 Da MWCO membrane and stirred in a large volume of the assembly buffer (100 mM Tris HCl pH 8.0, 5 mM $MgCl_2$) overnight. The solution within the microdialyzer was then removed and analyzed by 8% native PAGE (see Figure 6). A new, low-mobility band was clearly visible: control experiments confirmed that this new band was only seen when all four tetrahedron strands were present, indicating the successful formation of the polymer-conjugated DNA tetrahedron (see Figure S11, Supporting Information).

To further confirm that the observed product was indeed the polymer–tetrahedron conjugate, the possibility of attaching the polymer to an already assembled DNA nanostructure was explored. To achieve this, the s1, s2-alkyne, s3 and s4 strands were first phosphorylated using T4 polynucleotide kinase; the tetrahedron was then assembled using the normal thermal route. T4 DNA ligase was added to join the 3′ and 5′ ends of each strand to form four linked circles that lock the structure together topologically (this was desirable as the addition of organic solvents can cause the unligated tetrahedron to disassemble). Analysis by both native and denaturing PAGE confirmed the successful formation of the ligated tetrahedra (see Figure S12, Supporting Information).

Conjugation of the polymer was performed using standard water-based CuAAC reaction conditions.[51] The ligated tetrahedra were concentrated to approximately 1 μM, mixed with the azide-functionalized polymer (dissolved in degassed acetonitrile), $CuSO_4 \cdot 5H_2O$, (+)-sodium L-ascorbate, and tris-(hydroxypropyltriazolylmethyl)amine (THPTA) (all dissolved in degassed 18 MΩ water), and left overnight at 26 °C. Analysis of the reaction mixture by 8% native PAGE clearly showed the presence of a new band (Figure S13, Supporting Information), which corresponded exactly with that attributed to the polymer–tetrahedron conjugate in Figure 6. Since the ligated tetrahedron was incapable of disassembly, this confirmed that this band had been correctly assigned and that the conjugate had been successfully synthesized. It is worth noting that when the polymer was grafted to a preassembled tetrahedron, the yield of the tetrahedron–polymer conjugate was low; by contrast, when the tetrahedron was assembled using the s2-polymer species, the yield was close to quantitative. The latter is clearly the superior of the two approaches.

The concentration of the conjugate after assembly is far below the critical micelle concentration (CMC) usually observed for poly(NIPAM) nanostructures. However, it was hypothesized that, by heating the tetrahedron–poly(NIPAM) conjugate close to the cloud point of the polymer in the presence of a large background concentration of unfunctionalized poly(NIPAM), the collapse and aggregation of the polymer could be made to drive the formation of micelle-like structures with a hydrophobic poly(NIPAM) core and a hydrophilic corona composed of DNA tetrahedra. A solution of the tetrahedron–poly(NIPAM) (100 nM) was analyzed by DLS, both at room temperature and at 40 °C. The solution was cooled to room temperature, an aliquot of poly(NIPAM) homopolymer solution was added, and the measurements were repeated; this process was repeated several times until 10 equiv of the homopolymer had been added. At this maximum homopolymer concentration, DLS results indicated the formation of nanoparticles with a hydrodynamic diameter of around 220 nm at 40 °C, see Figure 7. These structures were not observed at room temperature, indicating that the temperature-responsive polymer was responsible for their formation. Further increasing the temperature of the solution above 40 °C led to an increase in the size of the structures (see Figure S14, Supporting Information). A possible cause of this phenomenon is the dynamic equilibrium between

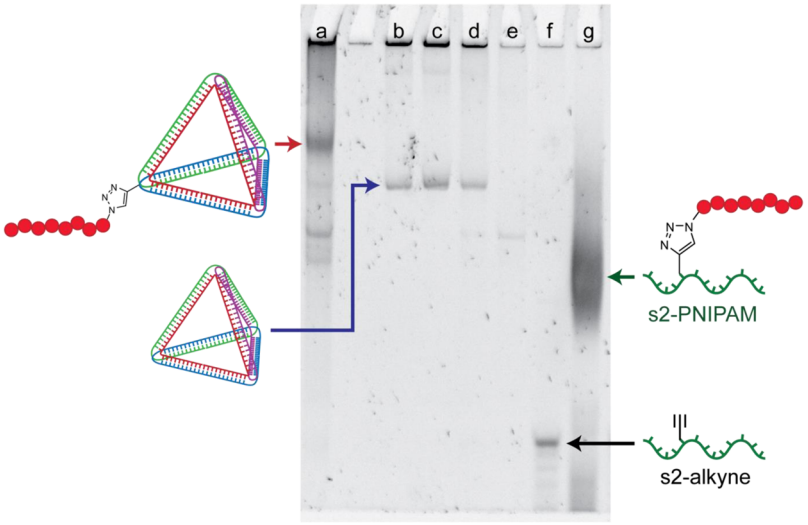

Figure 6. Tetrahedron–$PNIPAM_{45}$ conjugate analyzed by 8% native PAGE. Lane a, Tetrahedron–$PNIPAM_{45}$ conjugate; lane b, c, d, unfunctionalized DNA tetrahedra; lane e, s1 + s3 + s4; lane f, s2-alkyne; lane g, s2-$PNIPAM_{45}$.

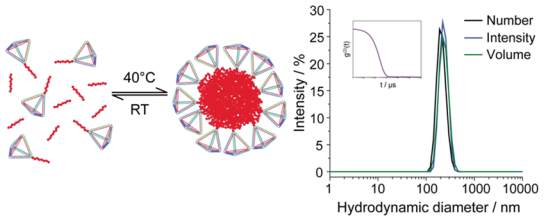

Figure 7. Temperature-induced formation of nanoparticles from poly(NIPAM)$_{45}$ in the presence of the DNA tetrahedron–poly(NIPAM) conjugate. Left: schematic of the proposed assembly process. Right: DLS data for the nanoparticles at 40 °C (correlation function inset); there was good agreement between the analyses by scattering intensity (blue), particle volume (green), and number of particles (black). The hydrodynamic diameter of the particles was estimated to be 220 nm, with a polydispersity of 0.13.

homopolymer free in solution and trapped in the core of the nanoparticles: as the temperature was increased, the equilibrium shifted to favor aggregation in the core, thus increasing the size of the particles. The homopolymer alone exhibited none of these properties: upon heating it simply aggregated and precipitated. The s2-poly(NIPAM) conjugate did exhibit the ability to form large structures under these conditions, but DLS indicated that they were unstable and the results were not reproducible. As a final control, unconjugated tetrahedra were mixed with poly(NIPAM) homopolymer and studied by DLS at 40 °C. Again, no stable structures were observed by DLS.

To corroborate the light scattering data, the nanoparticles were studied by cryogenic transmission electron microscopy (cryoTEM). Figure 8 shows a typical electron micrograph of one of the tetrahedron–poly(NIPAM) nanoparticles, as well as a particle size histogram (see Figure S15, Supporting Information for further cryoTEM images). The average particle size (79 ± 3 nm) is smaller than that observed by DLS (220 nm). The discrepancy likely arose because the light scattering method gave undue weight to the small but significant population of particles above 200 nm in diameter.

The nanoparticles were studied by AFM by drying them onto either a mica or glass surface to assess retention of conjugate-polymer associations in the presence of both a high and low energy substrate. On mica, DNA tetrahedron–polymer conjugates were observed both in isolation and in an aggregated state, with polymer distributed intermittently over the surface (see Supporting Information). In all images, both the DNA tetrahedron–polymer conjugates and the aggregates were found primarily on areas of the substrate covered by polymer. These results suggested that the mica induced the large hybrid nanoparticles to partially disassemble upon drying and that the resultant material is more stable on polymer than on a high-surface-energy substrate. On glass, a lower-surface-energy substrate, the strong preference for free polymer association to the DNA–polymer conjugates was more pronounced, with the polymer clustering around the DNA nanostructures (see Figure 8) and overall diameters of the DNA nanostructures and associated polymer approaching those observed in cryoTEM (see Figures S15 and S16, Supporting Information, for further AFM images and analysis). The differences in diameter can be attributed to the effects of drying the sample to the AFM substrate.

On the basis of the data from DLS, cryoTEM, and AFM, it is proposed that as the poly(NIPAM) homopolymer approached its cloud point, the formation of discrete nanoparticles (see Figure 7) composed of a collapsed polymer core stabilized by DNA nanostructures anchored to its surface by a covalently attached polymer chain was favored. As a result of the large volume occupied by the tetrahedron (relative to a single strand of DNA), only a low concentration of

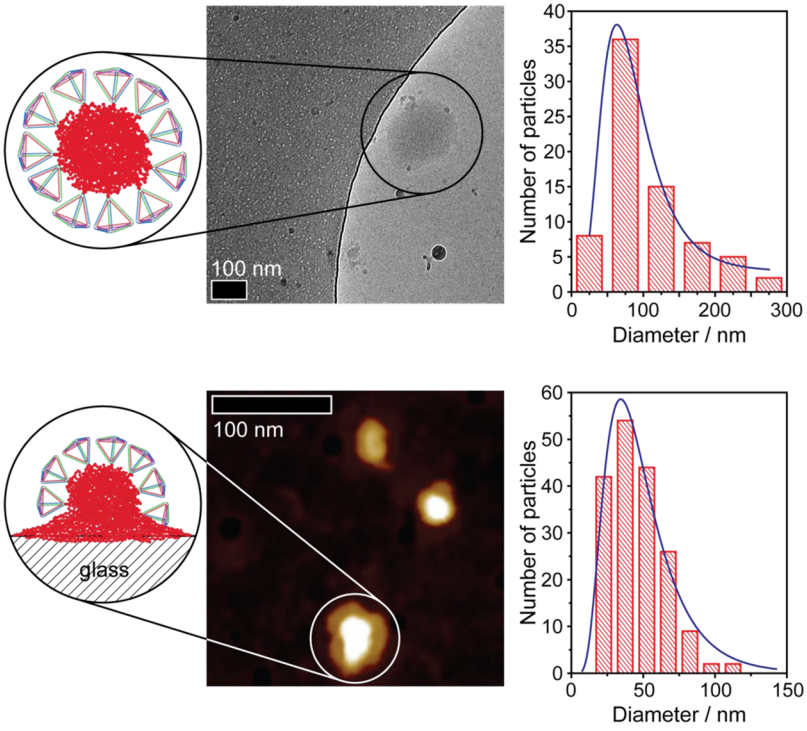

Figure 8. CryoTEM and AFM micrographs with particle analyses. Upper left: representative cryoTEM micrograph of a DNA tetrahedron–poly(NIPAM) nanoparticle. Upper right: particle size histogram (n = 73); log-normal fit provided (blue trace). Lower left: AFM micrograph of DNA tetrahedron–poly(NIPAM) nanoparticle and associated free polymer on glass. Lower right: particle diameter histogram (n = 178); log-normal fit provided (blue trace).

the conjugate was needed for stabilization to occur. The high density of negative charge on the DNA nanostructure prevented aggregation of the nanoparticles. The DNA tetrahedron–poly(NIPAM) species thus behaved like a"giant surfactant".

CONCLUSION

A fast and efficient solution-based route to DBCs by CuAAC has been identified. Since alkyne- and azide-functionalized DNAs are commercially available, and polymers end-modified with these reactive groups are already routinely synthesized by many research groups, it is hoped that the simplicity of the conjugation protocol will encourage greater exploration of the potential of DBCs by materials chemists. Given the huge variety of properties possessed by synthetic polymers, including pH- and redox-responsiveness, electrical conductivity, and catalysis, there are a number of exciting opportunities for the creation of materials with unique, useful, and interesting properties.

This work has demonstrated that an added layer of complexity can be introduced into DNA nanostructures by the addition of a responsive polymer block. We have created surfactant-like species capable of stabilizing hydrophobic polymer nanoparticles in aqueous solution at very high dilution. Future work will focus on exploitation of these temperature-responsive nanoparticles for a specific purpose: DNA tetrahedra in particular have been shown to effectively encapsulate proteins, including Cytochrome c[52] and a transcription factor,[53] so these hybrid structures could prove very useful in the fields of drug delivery and catalysis.[54–56] Given the almost bewildering array of shapes and architectures that can now be made using DNA self-assembly, functionalization of other DNA nanostructures with responsive polymers could lead to a vast number of novel materials.

MATERIALS AND METHODS

Materials. All DNA samples were purchased from Integrated DNA Technologies and used without further purification. T4 polynucleotide kinase and T4 DNA ligase were purchased from New England BioLabs, Inc., and used as received. 2-(Dodecylthiocarbonothioylthio)-2-methylpropionic acid (DDMAT), 3-azido-1-propanol, *N*-hexylpyridyl-methanimine (NHPMI), and copper iodide triethylphosphite (CuI·P(OEt)$_3$) were synthesized according to previously published procedures.[57–60] *N*-Isopropylacrylamide (NIPAM) was recrystallized from a mixture of toluene and hexane. α,α′-Azoisobutyronitrile (AIBN) was recrystallized from methanol. All other chemicals were purchased from Sigma Aldrich and used as received. DNA solution concentrations were determined using UV–vis absorption measurements at 260 nm. ^{1}H and ^{13}C NMR spectra were recorded on Bruker DPX-300 or -400 spectrometers at 293 K. Chemical shifts are reported as δ in parts per million (ppm) and referenced to the residual solvent resonances ($CDCl_3$ ^{1}H δ = 7.26 ppm; ^{13}C δ = 77.16 ppm). DMF SEC data were obtained in HPLC grade DMF containing 1 mg mL^{-1} of lithium bromide at 323 K, with a flow rate of 1.0 mL min^{-1}, on a set of two Varian PLgel 5 μm Mixed-D columns (7.5 mm diameter), with guard column.

SEC data were analyzed using Cirrus SEC software calibrated using poly(methyl methacrylate) standards (690−271 400 Da). ESI Mass spectra were collected on a Bruker Esquire2000 ESI-MS machine using methanol as solvent. UV−vis measurements were collected on a PerkinElmer Lambda 35 spectrometer using a Hellma TrayCell with a 1 mm path length adapter or, for cloud point measurements, with a quartz cell with a 1 cm path length. IR measurements were collected on a PerkinElmer Spectrum 100 FT-IR spectrometer. Native polyacrylamide gel electrophoresis (PAGE) was carried out with 1× Tris-Acetate EDTA (TAE) as running buffer at 4 °C and constant voltage of 200 V, loading with glycerol/bromophenol blue loading buffer. Denaturing PAGE was carried out using gels containing 8.3 M urea, with 1× Tris-Borate EDTA (TBE) as running buffer at a constant voltage of 300 V, loading with formamide/bromophenol blue/xylene cyanol loading buffer. All gels were run using a Bio-Rad Mini-Protean Tetra System apparatus and visualized using SybrGold nucleic acid stain, purchased from Invitrogen, under UV transillumination. Yields were estimated by densitometry using the Image-J image analysis package. HPLC analyses were performed on a Varian 920-LC integrated liquid chromatography system. Chromatography was performed on a Waters XBridgeOST C18 2.5 μm 4.6 × 50 mm column heated to 40 °C. Flow rate was set at 1 mL min^{-1} with a linear gradient of the following buffers: buffer A, 0.1 M triethylammonium acetate, 5% acetonitrile, pH 7.0; buffer B, 0.1 M triethylammonium acetate, 70% acetonitrile, pH 7.0. Fractions collected were combined and concentrated using an Eppendorf concentrator plus. For the assembly of tetrahedra, TEM buffer was used containing 10 mM Tris HCl pH 8.0, 1 mM EDTA and 6 mM $MgCl_2$. Hydrodynamic diameters (D_h) and size distributions of nanoparticles were determined by DLS on a Malvern Zetasizer Nano ZS operating at 24 or 40 °C with a 4 mW He−Ne 633 nm laser module. Disposable plastic sizing microcuvettes were used. Measurements were made at a detection angle of 173° (back scattering), and the data analyzed using Malvern DTS 6.20 software, using the multiple narrow modes setting. All measurements were made in triplicate, with at least 10 runs per measurement. Cryogenic transmission electron microscopy samples (100 nM in water) stabilized with citric acid (250 mM)[61] were examined using a Jeol 2010F TEM operated at 200 kV and imaged using a GatanUltrascan 4000 camera. Images were captured using Digital Micrograph software (Gatan). A 3 μL droplet of the sample solution held at 40 °C was rapidly transferred to a holey carbon-coated copper grid and blotted to remove excess solution. Subsequently, the grid was plunged into liquid ethane to vitrify the sample. The temperature of the cryogenic stage was maintained below −170 °C, using liquid nitrogen, during imaging. Where appropriate, particle size analysis was performed using ImageJ.

DNA Sequences. The following DNA sequences were used in this work. Unless otherwise stated, the sequences are given 5′ to 3′. The s0 strand was used for catalyst testing and was purchased with either an alkyne, azide, or amine modification at the 5′ end. The s1−s4 strands were the components of the DNA tetrahedron: for polymer conjugation, the s2 strand was ordered containing an alkyne-modified uracil residue as indicated below by U(alkyne). The color scheme used corresponds to that in the main article.

```
      s0: GCC CGA AAT ACC CCG TTA GAA A

      s1: AGG CAG TTG AGA CGA ACA TTC CTA AGT CTG AAA TTT ATC
          ACC CGC CAT AGT AGA CGT ATC ACC

      s2: CTT GCT ACA CGA TTC AGA CTT AGG AAT GTT CGA CAT GCG
          AGG GTC CAA TAC CGA CGA TTA CAG

s2-alkyne: CTT GCT ACA CGU(alkyne) TTC AGA CTT AGG AAT GTT CGA
          CAT GCG AGG GTC CAA TAC CGA CGA TTA CAG

      s3: GGT GAT AAA ACG TGT AGC AAG CTG TAA TCG ACG GGA AGA
          GCA TGC CCA TCC ACT ACT ATG GCG

      s4: CCT CGC ATG ACT CAA CTG CCT GGT GAT ACG AGG ATG GGC
          ATG CTC TTC CCG ACG GTA TTG GAC
```

Chain Transfer Agents. Three chain transfer agents (CTAs) were synthesized for this work, containing either an azide, alkyne, or pentafluorophenyl (PFP) activated ester group, as shown in Figure S1 (Supporting Information).

Perfluorophenyl 2-(dodecylthiocarbonothioylthio)-2-methylpropanoate, 1. The PFP-containing CTA **1** was prepared according to a previously published procedure.[32] DDMAT (0.5 g, 1.37 mmol) was added to an oven-dried Schlenk flask, which was then evacuated and refilled with nitrogen three times. Anhydrous DMF (7.5 mL) was added *via* syringe, and the flask was cooled to 0 °C with an ice bath. DIEA (354 μL, 2.74 mmol) was then added *via* syringe, followed by dropwise addition of pentafluorophenyl trifluoroacetate (283 μL, 1.65 mmol). After one hour stirring at 0 °C, the flask was opened to the air, and diethyl ether (30 mL) was added, followed by a 1 M solution of HCl (30 mL). The organic layer was collected and washed with water (2 × 30 mL) and brine (30 mL). The solvent was removed *in vacuo* to give a yellow oily residue, which was then purified by silica gel column chromatography, eluting with a mixture of ethyl acetate and pet. ether 40−60 (gradient from 5 to 10% ethyl acetate). The fractions containing the product (R_f 0.81) were combined and the solvent removed *in vacuo* to yield the product as a yellow oil (0.686 g, 94%). ^{1}H NMR (400 MHz, $CDCl_3$): δ 3.31 (t, J = 7 Hz, 2H, SCH_2), 1.86 (s, 6H, $C(CH_3)_2$), 1.69 (quint, J = 7 Hz, 2H, SCH_2CH_2), 1.40 (m, 2H, $SCH_2CH_2CH_2$), 1.26 (br s, 16H, $SCH_2CH_2(CH_2)_8$), 0.88 (t, J = 7 Hz, 3H, CH_2CH_3) ppm. ^{13}C NMR (150 MHz, $CDCl_3$): δ 219.9 (C=S), 169.6 (C=O), 142.1 (t), 140.4 (t), 138.7 (t), 137.0 (t) (PFP Cs), 55.4 ($C(CH_3)_2$), 37.2 (SCH_2), 31.9, 29.6, 29.5, 29.4, 29.3, 29.1, 29.0, 28.9, 27.8, 25.4 ($C(CH_3)_2$), 22.7 (CH_2CH_3), 14.1 ($S(CH_2)_{11}CH_3$) ppm. ^{19}F NMR (375 MHz, $CDCl_3$): δ −151.5 (d, 2F, ortho F), −157.7 (t, 2F, para F), −162.3 (t, 2F, meta F) ppm. IR (ν_{max}/cm^{-1}): 2925, 2854, 1779, 1517, 1079, 992, 815. ESI HR MS calcd. for $C_{23}H_{31}F_5O_2S_3$ $[M + H]^+$ 531.1486; observed 531.1480.

3-Azidopropyl 2-(dodecylthiocarbonothioylthio)-2-methylpropanoate, 2. The azide-containing CTA **2** was synthesized as follows. DDMAT (0.2 g, 0.55 mmol), EDCI·HCl (0.105 g, 0.55 mmol), and DMAP (0.006 g, 0.05 mmol) were dissolved in dichloromethane (2 mL) and stirred for one hour at room temperature. 3-Azido-1-propanol (0.05 g, 0.50 mmol) was then added, and the mixture was stirred for one week at room temperature. The solvent was then removed *in vacuo*, water (20 mL) was added, and the product was extracted into ethyl acetate (3 × 20 mL). The combined organic layers were washed with water (2 × 20 mL) and brine (20 mL) and finally dried with $MgSO_4$, which was then removed by filtration. The solvent was removed *in vacuo*, and the residue purified by silica gel column chromatography, eluting with a mixture of pet. ether 40−60 and ethyl acetate (9:1). The pure fractions (R_f 0.57) were combined, and the solvent removed to afford the product as a yellow oil (0.116 g, 52%). ^{1}H NMR (400 MHz, $CDCl_3$): δ 4.18 (t, J = 6 Hz, 2H, CH_2O), 3.36 (t, J = 7 Hz, 2H, CH_2N_3), 3.27 (t, J = 7 Hz, 2H, SCH_2), 1.90 (quint, J = 6 Hz, 2H, $CH_2CH_2N_3$), 1.69 (s, 6H, $C(CH_3)_2$), 1.66 (m, 2H, SCH_2CH_2), 1.38 (m, 2H, $SCH_2CH_2CH_2$), 1.34−1.21 (br m, 16H, $SCH_2CH_2CH_2(CH_2)_8CH_3$), 0.88 (t, J = 7 Hz, 3H, $S(CH_2)_{11}CH_3$) ppm. ^{13}C NMR (150 MHz, $CDCl_3$): δ 221.6 (C=S), 172.8 (C=O), 62.7 (OCH_2), 55.9 ($C(CH_3)_2$), 48.2 (CH_2N_3), 37.0 (SCH_2), 31.9, 29.6, 29.5, 29.4, 29.3, 29.1, 28.9, 28.0, 27.9, 25.4 ($C(CH_3)_2$), 22.7, 14.1 ($S(CH_2)_{11}CH_3$) ppm [Fewer signals are observed than expected because of overlap]. IR (ν_{max}/cm^{-1}): 2923, 2853, 2096, 1734, 1254, 1154, 1126, 1064, 814. ESI HR MS calcd. for $C_{20}H_{37}N_3O_2S_3$ $[M + Na]^+$ 470.1946; observed 470.1942.

***S*-Propargyloxycarbonylphenylmethyl dithiobenzoate, 3.** The alkyne-containing CTA **3** was prepared according to a previously published procedure.[34]

Poly(*N*-isopropylacrylamide). All polymers were synthesized using the same conditions: the only variables were the number of equivalents of monomer used, the CTA, and the reaction time. A representative procedure follows, using the PFP-containing CTA **1**. The CTA (0.094 g, 0.09 mmol), NIPAM (1 g, 8.84 mmol), and AIBN (0.003 g, 0.02 mmol) were dissolved in 1,4-dioxane (1.5 mL) and transferred to an oven-dried ampule. The mixture was subjected to three freeze−pump−thaw cycles and sealed under an atmosphere of nitrogen. It was then placed in an oil bath preheated to 65 °C. After 2 h, the ampule was removed, and the reaction quenched by opening it to air and cooling with liquid nitrogen. The solution was poured into pet. ether 40−60 (80 mL) cooled in an acetone/CO_2 bath, and the precipitant collected by filtration. The product was then dissolved in THF (1 mL), and the process repeated. The product

was isolated by filtration, dried *in vacuo*, and isolated as a yellow powder (0.521 g, 51%) and analyzed by DMF SEC using PMMA calibration standards (M_n 5 260 Da, Đ 1.10). ^{1}H NMR (400 MHz, $CDCl_3$): δ 7.40−5.70 (br m, pNIPAM N*H*), 4.00 (br s, pNIPAM C*H*$(CH_3)_2$), 3.35 (br m, 2H, SCH_2), 2.65−0.75 (br m, pNIPAM backbone *H*), 0.88 (t, J = 7 Hz, 3H, S$(CH_2)_{11}CH_3$) ppm. ^{19}F NMR (375 MHz, $CDCl_3$): δ −153.0 (br m, 2F, PFP end group ortho *F*), −158.0 (br m, 1F, PFP end group para *F*), −162.3 (br m, PFP end group meta *F*) ppm.

Analytical data for the poly(NIPAM) synthesized using the alkyne-functionalized CTA, **3**. ^{1}H NMR (400 MHz, $CDCl_3$): δ 7.94 (t, 2H, polymer end group Ar*H*), 7.54 (t, 1H, polymer end group Ar*H*), 7.37 (t, 2H, polymer end group Ar*H*), 7.32−7.14 (br m, polymer end group Ar*H*), 7.10−5.40 (br s, pNIPAM N*H*), 4.82−4.44 (br m, 2H, polymer end group CH_2C≡CH), 4.25−3.70 (br s, pNIPAM C*H*$(CH_3)_2$), 3.59 (br s, 1H, polymer end group C≡C*H*), 2.60−0.80 (br m, pNIPAM backbone *H*) ppm.

Poly(styrene). The polymerization of styrene was conducted as follows. CTA **3** (0.063 g, 0.19 mmol) was dissolved in styrene (1.1 mL, 9.60 mmol). The solution was transferred to an oven-dried ampule, which had been purged with nitrogen for 30 min. The mixture was subjected to five freeze−pump−thaw cycles and sealed under an atmosphere of nitrogen. It was then placed in an oil bath preheated to 110 °C and stirred for 28 h, after which time the reaction was allowed to cool to room temperature and poured into methanol (400 mL) cooled with dry ice. The product precipitated out and was collected by filtration, dissolved in a small amount of THF, and reprecipitated into cold methanol (200 mL), and finally collected by filtration as a pink solid (0.371 g, 48%), and analyzed by $CHCl_3$ SEC using PS standards (M_n 3 600, Đ 1.12). ^{1}H NMR (400 MHz, $CDCl_3$): δ 7.84 (br m, 2H, S═CAr*H*), 7.46 (br m, 1H, S═CAr*H*), 7.41−6.08 (br m, PS Ar*H*), 5.02−4.26 (br m, 3H, OCH_2C≡CH and SC*H*Ph), 3.23 (br s, 1H, C≡C*H*), 2.66−0.51 (br m, PS backbone *H*) ppm.

Poly(dimethylacrylamide). The polymerization of dimethylacrylamide (DMA) was conducted as follows. CTA **1** (53.5 mg, 0.10 mmol), DMA (1 g, 10.09 mmol) and AIBN (1.7 mg, 0.01 mmol) were dissolved in 1,4-dioxane (2 mL), and the mixture degassed by three successive freeze−pump−thaw cycles. The solution was sealed under a nitrogen atmosphere and placed in an oil bath preheated to 65 °C for four hours. After rapid cooling with liquid nitrogen to quench the polymerization, the flask was opened to air, and the solution added dropwise to a large volume of pet. ether 40−60 (300 mL). The precipitated product was collected by filtration as a yellow solid (0.871 g, 87%) and analyzed by DMF SEC using PMMA calibration standards (M_n 11.1 kDa, Đ 1.09). ^{1}H NMR (400 MHz, $CDCl_3$): δ 5.18 (m, 1H, SC*H*C═ONMe_2), 3.31 (m, 2H, SCH_2), 3.40−2.00 (br m, PDMA N$(CH_3)_2$ and C*H*C═ONMe_2), 2.00−1.00 (br m, PDMA backbone CH_2) ppm. ^{19}F NMR (375 MHz, $CDCl_3$): δ −153.0 (br m, 2F, PFP end group ortho *F*), −158.1 (br m, 1F, PFP end group para *F*), −162.3 (br m, PFP end group meta *F*) ppm.

Poly(4-acryloyl morpholine). The polymerization of 4-acryloyl morpholine (4-AM) was conducted as follows. CTA **1** (37.6 mg, 0.07 mmol), 4-AM (1 g, 7.08 mmol) and AIBN (1.2 mg, 0.01 mmol) were dissolved in 1,4-dioxane (3 mL), and the solution degassed by three successive freeze−pump−thaw cycles. The reaction mixture was sealed under a nitrogen atmosphere and placed in an oil bath preheated to 65 °C for four hours. After rapid cooling with liquid nitrogen to quench the polymerization, the flask was opened to air, and the solution added dropwise to a large volume of diethyl ether (200 mL) cooled in an ice bath. The precipitated product was collected by filtration and drying as a yellow solid (0.793 g, 82%) and analyzed by DMF SEC using PMMA calibration standards (M_n 9.3 kDa, Đ 1.11). ^{1}H NMR (400 MHz, $CDCl_3$): δ 5.16 (m, 1H, SC*H*C═ON), 4.00−3.00 (br m, P4-AM NCH_2CH_2), 2.90−1.00 (br m, P4-AM backbone *H*), 0.87 (t, 3H, S$(CH_2)_{11}CH_3$) ppm. ^{19}F NMR (375 MHz, $CDCl_3$): δ −153.3 (br m, 2F, PFP end group ortho *F*), −157.6 (br m, 1F, PFP end group para *F*), −161.9 (br m, PFP end group meta *F*) ppm.

End Group Removal. The trithiocarbonate group was removed[33] from the chain ends of poly(NIPAM), poly(DMA), and poly(4-AM) prior to further derivitization of the PFP group − an example procedure follows. Poly(NIPAM)-PFP (100 mg, 0.01 mmol), AIBN (187 mg, 1.14 mmol), and LPO (18 mg, 0.05 mmol) were dissolved in dry toluene (28 mL), and the solution degassed by three freeze−pump−thaw cycles and then sealed under nitrogen. The mixture was heated to 80 °C for five hours and then allowed to cool to room temperature. The solvent was removed *in vacuo*, and the residue resuspended in THF (1 mL), which was then poured into pet. ether 40−60 (15 mL) cooled with an ice bath. The precipitated product was collected by filtration and dried under vacuum to give a white powder (71 mg, 71%), which was analyzed by DMF SEC using PMMA calibration standards (M_n 8.2 kDa, Đ 1.11). ^{1}H NMR (400 MHz, $CDCl_3$): δ 8.00−5.50 (br m, pNIPAM N*H*), 4.00 (br s, pNIPAM C*H*$(CH_3)_2$), 3.00−0.50 (br m, pNIPAM backbone *H*) ppm. ^{19}F NMR (375 MHz, $CDCl_3$): δ −153.0 (br m, 2F, PFP end group F_{ortho}), −158.0 (br m, 1F, PFP end group F_{para}), −162.3 (br m, 2F, PFP end group F_{meta}) ppm.

End Group Modification. The PFP polymer end group was substituted with 3-azido-1-aminopropane as follows, using a modified literature procedure.[62] An example procedure follows: the same technique was used to introduce an azide group into the chain ends of poly(DMA) and poly(4-AM). Poly(NIPAM) (M_n 8.2 kDa, Đ 1.11) (40.0 mg, 5 μmol), 3-azido-1-aminopropane (2.4 mg, 24 μmol), and TEA (1.2 mg, 12 μmol) were dissolved in anhydrous THF (0.5 mL) under nitrogen in an oven-dried ampule. The solution was degassed by three successive freeze−pump−thaw cycles, then heated to 35 °C for two hours, and then for a further 15 h at room temperature. Water (10 mL) was added, and the mixture dialyzed against 18 MΩ water (MWCO 1 kDa), with six water changes, to remove excess small molecules. The product was isolated by freeze-drying as a white solid (21 mg, 53%) and analyzed by DMF SEC using PMMA calibration standards (M_n 8.0 kDa, Đ 1.09). ^{1}H NMR (400 MHz, $CDCl_3$): δ 7.20−5.50 (br m, pNIPAM N*H*), 4.00 (br s, pNIPAM C*H*$(CH_3)_2$), 3.42−3.21 (br m, 4H, CONHCH_2 and CH_2N_3), 2.80−0.5 (br m, pNIPAM backbone *H*) ppm. IR (ν_{max}/cm^{-1}): 3296, 2971, 2100 (N_3 stretch), 1639, 1535, 1458.

DNA−Polymer Conjugates. DMF was degassed by bubbling with N_2 for 30 min prior to use. DMF (75 μL), poly(NIPAM)-N_3 (10 μL, 1 mM in DMF), CuI·P$(OEt)_3$ (10 μL, 1 mM in DMF), and s2-alkyne DNA (5 μL, 200 μM in water) were mixed in a centrifuge tube and left at room temperature overnight. The reaction mixture was then concentrated *in vacuo* to a final volume of approximately 10 μL. HPLC buffer A (90 μL) was added, and the mixture was vortexed and then centrifuged. The s2-poly(NIPAM) conjugate was identified by 15% native PAGE and isolated by HPLC (see Figure S10, Supporting Information). After resuspension of the dried fractions in 18 MΩ water, the yield was estimated to be 50% by UV−vis spectroscopy.

Degradation of the Azide Group under RAFT Conditions. To measure the resistance of the azide group to RAFT polymerization conditions, poly(NIPAM) was synthesized using CTA **2** with a molecular weight of 7.8 kDa and a PDI of 1.13 (DMF SEC, PMMA calibration standards). The FTIR spectrum was recorded and compared with that of a poly(NIPAM) sample of similar molecular weight in which the azide group had been introduced postpolymerization. The azide group exhibits a characteristic peak at 2100 cm^{-1}.

Catalyst Testing. All solvents were degassed by bubbling with N_2 for 30 min prior to use. The catalyst/ligand (1.0 μL, 2 mM in the reaction solvent), polymer (1.0 μL, 2 mM in the reaction solvent) and DNA (0.5 μL, 200 μM in water) solutions were mixed in a centrifuge tube, and the volume topped up to 10 μL with the reaction solvent. The tube was closed, briefly vortexed and then left overnight. The yield of the DNA−polymer conjugate was assessed by 15% native PAGE analysis.

Degassing of the reaction solvent is important for the CuAAC reaction to proceed properly. The presence of oxygen leads to the Cu(I) source catalyzing the Glaser coupling, resulting in dimerization of the alkyne DNA.

Ligation of the DNA Tetrahedron. The alkyne-functionalized DNA tetrahedron was assembled and ligated as follows. DNA strands s1, s2-alkyne, s3, and s4 (1 μL of each, 10 μM in water) were mixed with 18 MΩ water (84 μL), 10× T4 DNA ligase buffer (10 μL), and T4 polynucleotide kinase (2 μL, 10 000 units mL^{-1}), and the solution heated at 37 °C for 30 min. The temperature was then increased to 65 °C for 20 min to deactivate the enzyme.

The temperature was again increased, to 95 °C, for 4 min, after which time the solution was cooled rapidly by submersing the reaction vessel in an ice bath. Once cool, T4 DNA ligase (5 μL, 400 000 cohesive end units mL^{-1}) was added, and the mixture incubated at room temperature for one hour. Analysis by 8% native PAGE confirmed the successful formation of the tetrahedron, and denaturing PAGE confirmed that the ligation procedure had been successful (see Figure S12, Supporting Information): native PAGE confirmed the successful formation of the tetrahedral structure; the resistance of the tetrahedra to denaturing conditions confirmed that they had been successfully ligated and that a topologically locked structure had been formed.

Attachment of Poly(NIPAM) to the Ligated DNA Tetrahedron. All solutions were degassed by bubbling with nitrogen for 30 min prior to use. The ligated tetrahedron (20 μL, 250 nM in TEM buffer), azide-functionalized poly(NIPAM)$_{45}$ (10 μL, 10 mM in acetonitrile), copper sulfate pentahydrate (10 μL, 10 mM in water), (+)-sodium L-ascorbate (10 μL, 10 mM in water), and tris-(hydroxypropyltriazolylmethyl)amine (THPTA) (10 μL, 10 mM in water) were mixed and left overnight at 26 °C. Analysis by 8% native PAGE confirmed that the tetrahedron−polymer conjugate had been formed in approximately 40% yield (see Figure S13, Supporting Information).

Measurement of the Cloud Point of Poly(NIPAM)$_{45}$. The cloud point of the poly(NIPAM) homopolymer was measured by following the UV−vis absorbance. A solution of the homopolymer (0.8 mg mL^{-1} in 1× TEM buffer) was heated in a quartz cuvette within a UV−vis spectrometer, and the absorbance followed at 500 nm (see Figure S3, Supporting Information) from 20 to 60 °C. After normalization of the maximum absorbance to one, the cloud point was taken as the temperature at which the absorbance was 0.5. This was found to be at 42 °C.

Self-Assembly of Poly(NIPAM)$_{45}$ in the Presence of the Tetrahedron−Poly(NIPAM) Conjugate. Hybrid nanoparticles were produced as follows. A solution of the tetrahedron−poly(NIPAM) conjugate (60 μL, 100 nM in 1X TEM buffer) was added to a DLS cuvette, and the light scattering data recorded at 25 °C. The temperature was then increased to 40 °C, and the measurement repeated. After cooling to 25 °C, an aliquot of poly(NIPAM)$_{45}$ homopolymer (0.8 mg mL^{-1} in TEM buffer) was added, the sample was allowed to equilibrate for 2 min, and the DLS measurement taken. The temperature was then increased to 40 °C, and the measurement repeated. This process was iterated until data had been acquired for the addition of 0.1, 0.5, 1, 2, 5, and 10 equiv of homopolymer (relative to the tetrahedron−poly(NIPAM) conjugate).

To ascertain whether the tetrahedron structure was responsible for the stabilization of the nanoparticles, the experiment was repeated using the s2-poly(NIPAM) conjugate. In place of the DNA tetrahedron, the DNA component of this species is a single strand without designed secondary structure. DLS indicated the formation of large, unstable particles ranging in diameter from around 50 to 500 nm.

To check that the homopolymer did not form structures on its own, a solution of poly(NIPAM)$_{45}$ was heated to 40 °C, and a DLS measurement was taken. Even after extended equilibration at this temperature, only macroscopic aggregates were observed, suggesting that the polymer does not form any sort of well-defined nanostructure.

Conflict of Interest: The authors declare no competing financial interest.

Acknowledgment. We thank Joseph Patterson (University of Warwick) for invaluable help with electron microscopy and Dr. Eugen Stultz (University of Southampton) and Dr. Mireya McKee (University of Oxford) for useful discussions. T.R.W. would like to thank the Warwick Chancellor's Scholarship for funding and also the ESF P2M network. The SEC used in this research was obtained through Birmingham Science City: Innovative Uses for Advanced Materials in the Modern World with support from Advantage West Midlands (AWM) and partially funded by the European Regional Development Fund (ERDF). This research was funded by EPSRC Grant EP/G037930/1. A.J.T. is supported by a Royal Society−Wolfson Research Merit Award.

Supporting Information Available: Detailed experimental procedures, full characterization data for all compounds, and additional microscopy images. This material is available free of charge *via* the Internet at http://pubs.acs.org.

REFERENCES AND NOTES

1. Seeman, N. C. Nucleic Acid Junctions and Lattices. *J. Theor. Biol.* **1982**, *99*, 237–247.
2. Rothemund, P. W. K. Folding DNA to Create Nanoscale Shapes and Patterns. *Nature* **2006**, *440*, 297–302.
3. Liu, D.; Balasubramanian, S. A Proton-Fuelled DNA Nanomachine. *Angew. Chem., Int. Ed.* **2003**, *42*, 5734–5736.
4. Modi, S.; Swetha, M. G.; Goswami, D.; Gupta, G. D.; Mayor, S.; Krishnan, Y. A DNA Nanomachine that Maps Spatial and Temporal pH Changes Inside Living Cells. *Nat. Nanotechnol.* **2009**, *4*, 325–330.
5. Andersen, E. S.; Dong, M.; Nielsen, M. M.; Jahn, K.; Subramani, R.; Mamdouh, W.; Golas, M. M.; Sander, B.; Stark, H.; Oliveira, C. L. P.; *et al.* Self-Assembly of a Nanoscale DNA Box with a Controllable Lid. *Nature* **2009**, *459*, 73–76.
6. Goodman, R. P.; Heilemann, M.; Doose, S.; Erben, C. M.; Kapanidis, A. N.; Turberfield, A. J. Reconfigurable, Braced, Three-Dimensional DNA Nanostructures. *Nat. Nanotechnol.* **2008**, *3*, 93–96.
7. Zheng, J.; Birktoft, J. J.; Chen, Y.; Wang, T.; Sha, R.; Constantinou, P. E.; Ginell, S. L.; Mao, C.; Seeman, N. C. From Molecular to Macroscopic *via* the Rational Design of a Self-Assembled 3D DNA Crystal. *Nature* **2009**, *461*, 74–77.
8. Winfree, E.; Liu, F.; Wenzler, L. A.; Seeman, N. C. Design and Self-Assembly of Two-Dimensional DNA Crystals. *Nature* **1998**, *394*, 539–544.
9. Douglas, S. M.; Bachelet, I.; Church, G. M. A Logic-Gated Nanorobot for Targeted Transport of Molecular Payloads. *Science* **2012**, *335*, 831–834.
10. Seelig, G.; Soloveichik, D.; Zhang, D. Y.; Winfree, E. Enzyme-Free Nucleic Acid Logic Circuits. *Science* **2006**, *314*, 1585–1588.
11. Qian, L.; Winfree, E. Scaling Up Digital Circuit Computation with DNA Strand Displacement Cascades. *Science* **2011**, *332*, 1196–1201.
12. Hawker, C. J. Molecular Weight Control by a "Living" Free-Radical Polymerization Process. *J. Am. Chem. Soc.* **1994**, *116*, 11185–11186.
13. Matyjaszewski, K.; Gaynor, S.; Wang, J.-S. Controlled Radical Polymerizations: The Use of Alkyl Iodides in Degenerative Transfer. *Macromolecules* **1995**, *28*, 2093–2095.
14. Moad, G.; Rizzardo, E.; Thang, S. H. Living Radical Polymerization by the RAFT Process. *Aust. J. Chem.* **2005**, *58*, 379–410.
15. Patra, S. K.; Ahmed, R.; Whittell, G. R.; Lunn, D. J.; Dunphy, E. L.; Winnik, M. A.; Manners, I. Cylindrical Micelles of Controlled Length with a π-Conjugated Polythiophene Core *via* Crystallization-Driven Self-Assembly. *J. Am. Chem. Soc.* **2011**, *133*, 8842–8845.
16. Gilroy, J. B.; Gädt, T.; Whittell, G. R.; Chabanne, L.; Mitchels, J. M.; Richardson, R. M.; Winnik, M. A.; Manners, I. Monodisperse Cylindrical Micelles by Crystallization-Driven Living Self-Assembly. *Nat. Chem.* **2010**, *2*, 566–570.
17. Brinkhuis, R. P.; Rutjes, F. P. J. T.; van Hest, J. C. M. Polymeric Vesicles in Biomedical Applications. *Polym. Chem.* **2011**, *2*, 1449–1462.
18. Stuart, M. A. C.; Huck, W. T. S.; Genzer, J.; Muller, M.; Ober, C.; Stamm, M.; Sukhorukov, G. B.; Szleifer, I.; Tsukruk, V. V.; Urban, M.; *et al.* Emerging Applications of Stimuli-Responsive Polymer Materials. *Nat. Mater.* **2010**, *9*, 101–113.
19. Alarcon, C.; de la, H.; Pennadam, S.; Alexander, C. Stimuli Responsive Polymers for Biomedical Applications. *Chem. Soc. Rev.* **2005**, *34*, 276–285.
20. Ganta, S.; Devalapally, H.; Shahiwala, A.; Amiji, M. A Review of Stimuli-Responsive Nanocarriers for Drug and Gene Delivery. *J. Controlled Release* **2008**, *126*, 187–204.
21. Alemdaroglu, F. E.; Herrmann, A. DNA Meets Synthetic Polymers—Highly Versatile Hybrid Materials. *Org. Biomol. Chem.* **2007**, *5*, 1311–1320.

22. Kwak, M.; Herrmann, A. Nucleic Acid/Organic Polymer Hybrid Materials: Synthesis, Superstructures, and Applications. *Angew. Chem., Int. Ed.* **2010**, *49*, 8574–8587.
23. Alemdaroglu, F. E.; Ding, K.; Berger, R.; Herrmann, A. DNA-Templated Synthesis in Three Dimensions: Introducing a Micellar Scaffold for Organic Reactions. *Angew. Chem., Int. Ed.* **2006**, *45*, 4206–4210.
24. Alemdaroglu, F. E.; Alemdaroglu, N. C.; Langguth, P.; Herrmann, A. DNA Block Copolymer Micelles—A Combinatorial Tool for Cancer Nanotechnology. *Adv. Mater.* **2008**, *20*, 899–902.
25. Li, Z.; Zhang, Y.; Fullhart, P.; Mirkin, C. A. Reversible and Chemically Programmable Micelle Assembly with DNA Block-Copolymer Amphiphiles. *Nano Lett.* **2004**, *4*, 1055–1058.
26. Chien, M.-P.; Rush, A. M.; Thompson, M. P.; Gianneschi, N. C. Programmable Shape-Shifting Micelles. *Angew. Chem., Int. Ed.* **2010**, *49*, 5076–5080.
27. Zhao, Z.; Wang, L.; Liu, Y.; Yang, Z.; He, Y.-M.; Li, Z.; Fan, Q.-H.; Liu, D. pH-Induced Morphology-Shifting of DNA-*b*-Poly(Propylene Oxide) Assemblies. *Chem. Commun.* **2012**, *48*, 9753–9755.
28. Carneiro, K. M. M.; Hamblin, G. D.; Hanni, K. D.; Fakhoury, J.; Nayak, M. K.; Rizis, G.; McLaughlin, C. K.; Bazzi, H. S.; Sleiman, H. F. Stimuli-Responsive Organization of Block Copolymers on DNA Nanotubes. *Chem. Sci.* **2012**, *3*, 1980–1986.
29. McLaughlin, C. K.; Hamblin, G. D.; Hänni, K. D.; Conway, J. W.; Nayak, M. K.; Carneiro, K. M. M.; Bazzi, H. S.; Sleiman, H. F. Three-Dimensional Organization of Block Copolymers on "DNA-Minimal" Scaffolds. *J. Am. Chem. Soc.* **2012**, *134*, 4280–4286.
30. Goodman, R. P.; Schaap, I. A. T.; Tardin, C. F.; Erben, C. M.; Berry, R. M.; Schmidt, C. F.; Turberfield, A. J. Rapid Chiral Assembly of Rigid DNA Building Blocks for Molecular Nanofabrication. *Science* **2005**, *310*, 1661–1665.
31. Ladmiral, V.; Legge, T. M.; Zhao, Y.; Perrier, S. b. "Click" Chemistry and Radical Polymerization: Potential Loss of Orthogonality. *Macromolecules* **2008**, *41*, 6728–6732.
32. Godula, K.; Rabuka, D.; Nam, K. T.; Bertozzi, C. R. Synthesis and Microcontact Printing of Dual End-Functionalized Mucin-like Glycopolymers for Microarray Applications. *Angew. Chem., Int. Ed.* **2009**, *48*, 4973–4976.
33. Chen, M.; Moad, G.; Rizzardo, E. Thiocarbonylthio End Group Removal from RAFT-Synthesized Polymers by a Radical-Induced Process. *J. Polym. Sci., Part A: Polym. Chem.* **2009**, *47*, 6704–6714.
34. O'Reilly, R. K.; Joralemon, M. J.; Hawker, C. J.; Wooley, K. L. Facile Syntheses of Surface-Functionalized Micelles and Shell Cross-Linked Nanoparticles. *J. Polym. Sci., Part A: Polym. Chem.* **2006**, *44*, 5203–5217.
35. Scarpa, J. S.; Mueller, D. D.; Klotz, I. M. Slow Hydrogen-Deuterium Exchange in a Non-α-Helical Polyamide. *J. Am. Chem. Soc.* **1967**, *89*, 6024–6030.
36. Schild, H. G. Poly(*N*-Isopropylacrylamide): Experiment, Theory and Application. *Prog. Polym. Sci.* **1992**, *17*, 163–249.
37. Costioli, M. D.; Fisch, I.; Garret-Flaudy, F.; Hilbrig, F.; Freitag, R. DNA Purification by Triple-Helix Affinity Precipitation. *Biotechnol. Bioeng.* **2003**, *81*, 535–545.
38. Umeno, D.; Maeda, M. Poly(*N*-Isopropylacrylamide) Carrying Double-Stranded DNA for Affinity Separation of Genotoxins. *Anal. Sci.* **1997**, *13*, 553–556.
39. Ayaz, M. S.; Kwak, M.; Alemdaroglu, F. E.; Wang, J.; Berger, R.; Herrmann, A. Synthesis of DNA Block Copolymers with Extended Nucleic Acid Segments by Enzymatic Ligation: Cut and Paste Large Hybrid Architectures. *Chem. Commun.* **2011**, *47*, 2243–2245.
40. Maeda, M.; Nishimura, C.; Inenaga, A.; Takagi, M. Modification of DNA with Poly(*N*-Isopropylacrylamide) for Thermally Induced Affinity Separation. *React. Polym.* **1993**, *21*, 27–35.
41. Murata, M.; Kaku, W.; Anada, T.; Sato, Y.; Kano, T.; Maeda, M.; Katayama, Y. Novel DNA/Polymer Conjugate for Intelligent Antisense Reagent with Improved Nuclease Resistance. *Bioorg. Med. Chem . Lett.* **2003**, *13*, 3967–3970.
42. Sugawara, Y.; Tamaki, T.; Ohashi, H.; Yamaguchi, T. Control of the Poly(*N*-Isopropylacrylamide) Phase Transition *via* a Single Strand-Double Strand Transformation of Conjugated DNA. *Soft Matter* **2013**, *9*, 3331–3340.
43. Bock, V. D.; Hiemstra, H.; van Maarseveen, J. H. CuI-Catalyzed Alkyne−Azide "Click" Cycloadditions from a Mechanistic and Synthetic Perspective. *Eur. J. Org. Chem.* **2006**, 51–68.
44. El-Sagheer, A. H.; Brown, T. Click Chemistry with DNA. *Chem. Soc. Rev.* **2010**, *39*, 1388–1405.
45. Dallmann, A.; El-Sagheer, A. H.; Dehmel, L.; Mügge, C.; Griesinger, C.; Ernsting, N. P.; Brown, T. Structure and Dynamics of Triazole-Linked DNA: Biocompatibility Explained. *Chem.—Eur. J.* **2011**, *17*, 14714–14717.
46. Presolski, S. I.; Hong, V.; Cho, S.-H.; Finn, M. G. Tailored Ligand Acceleration of the Cu-Catalyzed Azide−Alkyne Cycloaddition Reaction: Practical and Mechanistic Implications. *J. Am. Chem. Soc.* **2010**, *132*, 14570–14576.
47. Safak, M.; Alemdaroglu, F. E.; Li, Y.; Ergen, E.; Herrmann, A. Polymerase Chain Reaction as an Efficient Tool for the Preparation of Block Copolymers. *Adv. Mater.* **2007**, *19*, 1499–1505.
48. Rush, A. M.; Thompson, M. P.; Tatro, E. T.; Gianneschi, N. C. Nuclease Resistant DNA *via* High-Density Packing in Polymeric Micellar Nanoparticle Coronas. *ACS Nano* **2013**, *7*, 1379–1387.
49. Patterson, J. P.; Sanchez, A. M.; Petzetakis, N.; Smart, T. P.; Epps, T. H., III.; Portman, I.; Wilson, N. R.; O'Reilly, R. K. A Simple Approach to Characterizing Block Copolymer Assemblies: Graphene Oxide Supports for High Contrast Multi-Technique Imaging. *Soft Matter* **2012**, *8*, 3322–3328.
50. Jungmann, R.; Liedl, T.; Sobey, T. L.; Shih, W.; Simmel, F. C. Isothermal Assembly of DNA Origami Structures Using Denaturing Agents. *J. Am. Chem. Soc.* **2008**, *130*, 10062–10063.
51. Averick, S.; Paredes, E.; Li, W.; Matyjaszewski, K.; Das, S. R. Direct DNA Conjugation to Star Polymers for Controlled Reversible Assemblies. *Bioconjugate Chem.* **2011**, *22*, 2030–2037.
52. Erben, C. M.; Goodman, R. P.; Turberfield, A. J. Single-Molecule Protein Encapsulation in a Rigid DNA Cage. *Angew. Chem., Int. Ed.* **2006**, *45*, 7414–7417.
53. Crawford, R.; Erben, C. M.; Periz, J.; Hall, L. M.; Brown, T.; Turberfield, A. J.; Kapanidis, A. N. Non-Covalent Single Transcription Factor Encapsulation Inside a DNA Cage. *Angew. Chem., Int. Ed.* **2013**, *52*, 2284–2288.
54. Walsh, A. S.; Yin, H.; Erben, C. M.; Wood, M. J. A.; Turberfield, A. J. DNA Cage Delivery to Mammalian Cells. *ACS Nano* **2011**, *5*, 5427–5432.
55. Jiang, Q.; Song, C.; Nangreave, J.; Liu, X.; Lin, L.; Qiu, D.; Wang, Z.-G.; Zou, G.; Liang, X.; Yan, H.; *et al.* DNA Origami as a Carrier for Circumvention of Drug Resistance. *J. Am. Chem. Soc.* **2012**, *134*, 13396–13403.
56. Lee, H.; Lytton-Jean, A. K. R.; Chen, Y.; Love, K. T.; Park, A. I.; Karagiannis, E. D.; Sehgal, A.; Querbes, W.; Zurenko, C. S.; Jayaraman, M.; *et al.* Molecularly Self-Assembled Nucleic Acid Nanoparticles for Targeted *in vivo* siRNA Delivery. *Nat. Nanotechnol.* **2012**, *7*, 389–393.
57. Skey, J.; O'Reilly, R. K. Facile One Pot Synthesis of a Range of Reversible Addition-Fragmentation Chain Transfer (RAFT) Agents. *Chem. Commun.* **2008**, 4183–4185.
58. Scheel, A. J.; Komber, H.; Voit, B. I. Novel Hyperbranched Poly([1,2,3]-triazole)s Derived from AB_2 Monomers by a 1,3-Dipolar Cycloaddition. *Macromol. Rapid Commun.* **2004**, *25*, 1175–1180.
59. Haddleton, D. M.; Crossman, M. C.; Dana, B. H.; Duncalf, D. J.; Heming, A. M.; Kukulj, D.; Shooter, A. J. Atom Transfer Polymerization of Methyl Methacrylate Mediated by Alkylpyridylmethanimine Type Ligands, Copper(I) Bromide, and Alkyl Halides in Hydrocarbon Solution. *Macromolecules* **1999**, *32*, 2110–2119.
60. Ziegler, F. E.; Fowler, K. W.; Rodgers, W. B.; Wester, R. T. Ambient Temperature Ullmann Reaction: 4,5,4′,5′-Tetramethoxy-1,1′-biphenyl-2,2′-dicarboxaldehyde. *Org. Synth.* **1987**, *65*, 108–118.

61. Moughton, A. O.; Patterson, J. P.; O'Reilly, R. K. Reversible Morphological Switching of Nanostructures in Solution. *Chem. Commun.* **2011**, *47*, 355–357.
62. Wiss, K. T.; Theato, P. Facilitating Polymer Conjugation *via* Combination of RAFT Polymerization and Activated Ester Chemistry. *J. Polym. Sci., Part A: Polym. Chem.* **2010**, *48*, 4758–4767.